# Raman Spectroscopic Study of Co–Mo/γ-Al₂O₃ Catalysts

J. MEDEMA,* C. VAN STAM,* V. H. J. DE BEER,† A. J. A. KONINGS,†
AND D. C. KONINGSBERGER†

*Chemical Laboratory, National Defence Research Organisation TNO, Lange Kleiweg 137, Rijswijk (Z.H.),
and †Department of Inorganic Chemistry and Catalysis, Eindhoven University of Technology,
Eindhoven, The Netherlands

Laser Raman spectroscopy is used to study the structure of molybdenum and cobalt species present in Co–Mo/γ-Al₂O₃ catalyst systems. From comparison with Raman spectra of Mo and Co in known structures it is derived that these catalyst systems contain Mo and Co in different modifications depending on the degree of surface coverage. In the absence of Co, four different Mo species are found. At low coverages isolated molybdate tetrahedra are observed. Increasing the surface coverage results in formation of a polymolybdate phase in which Mo is octahedrally surrounded. At higher coverages "bulk" aluminum molybdate is formed. At very high coverages formation of "free" MoO₃ occurs. In Co/γ-Al₂O₃ samples the color indicates the presence of Co₃O₄- and CoAl₂O₄-like species. When Co is introduced in Mo/γ-Al₂O₃ (Co/Mo atomic ratio, 0.64) various effects occur. "Free" MoO₃, as well as Al₂(MoO₄)₃, is converted into "CoMoO₄." Cobalt addition results in a decrease of the isolated Mo tetrahedra concentration in favor of the polymeric molybdate form, which apparently is not qualitatively affected by the presence of Co. In Co–Mo/γ-Al₂O₃ most of the Co is present in a structure comparable to CoAl₂O₄. The influences of the nature of the support, heat treatment, reduction in hydrogen and the effect of sulfiding are discussed briefly.

## INTRODUCTION

Oxidic Co–Mo/γ-Al₂O₃ is the precursor of a widely used hydrodesulfurization (HDS) catalyst (1–5). As the interaction between the precursor and sulfur in various chemical forms is an essential step in the formation of the actual active (sulfided) catalyst modification, this oxidic catalyst system was selected for the study of the decomposition of dichlorodiethyl sulfide (mustard gas). From infrared spectroscopic data the structure of mustard gas adsorbed on the catalyst surface could be derived (6). Because the catalyst was found not to be transparent in the spectral region below 1000 cm⁻¹, an attempt was made to obtain more insight into the behavior of the C–Cl and C–S–C vibrations by means of Raman spectroscopy. However, it appeared that the background spectrum due to cobalt and molybdenum obscured to a large extent the Raman spectrum of adsorbed species. Moreover, it appeared that the background spectrum showed considerable changes when changing the composition of the catalyst. From these observations it was concluded that Raman spectroscopy might be a useful experimental tool to study the structure of Mo and Co species present in oxidic and sulfided HDS catalysts.

The use of Raman spectroscopy to study catalyst structures has been reviewed by

Cooney *et al.* *(7)*. Oganowski *et al.* *(8)*, Müller *et al.* *(9)*, and Leroy *et al.* *(10)* have demonstrated that by means of Raman spectroscopy valuable information concerning the structure of Mo- or W-containing species can be obtained. $MoS_2$ *(11, 12)* and $MoS_3$ *(13)* have also been studied. In the case of oxidic and sulfided Co–Mo/$\gamma$-Al₂O₃ or related HDS catalyst systems only a few laser Raman studies are reported in the literature and the results obtained are conflicting. Villa *et al.* *(14)* state that Mo/$\gamma$-Al₂O₃ and Co–Mo/$\gamma$-Al₂O₃ samples do not contain Raman-active Mo and/or Co compounds. Pott and Stork *(15)* have reported successful application of Raman spectroscopy in an investigation on the structure of W/$\gamma$-Al₂O₃ catalysts. After completion of the experimental part of our Raman study, Brown and Makovsky *(16)* published spectra of oxidic and sulfided Co–Mo/$\gamma$-Al₂O₃, $MoO_3$ and $MoS_2$. These authors have found the presence of "free" $MoO_3$ and $CoMoO_4$ in oxidic Co–Mo/$\gamma$-Al₂O₃ to be unlikely. In sulfided catalysts they showed that at least part of the Mo is present as $MoS_2$. No explicit interpretation for the observed Mo–O stretching vibrations was given.

Since the combined data published so far in many papers *(1–5)* dealing with the structure of oxidic Co–Mo/$\gamma$-Al₂O₃ catalyst systems still do not give a complete picture of the Mo and Co species present in these HDS catalyst precursors, a Raman study concentrating mainly on oxidic samples was begun.

In the present investigation four different carrier materials have been used. These comprised two types of alumina: (i) one having a low specific surface area but especially suited for Raman spectroscopy because of a low fluorescence level and (ii) a typical HDS base alumina. Two silicas have also been used, mainly for comparison. These carriers were impregnated with various amounts of molybdenum and/or cobalt. Structural changes

with composition have been studied. In order to interpret the results obtained for the supported samples, the Raman spectra of pure compounds of known structure have also been recorded.

## EXPERIMENTAL METHODS

*Materials.* (a) $\gamma$-Alumina (Degussa, Type C) with a specific surface area of 80 m² g⁻¹ was used as a carrier material. It has favorable properties for recording Raman spectra because the fluorescence in this type of alumina is found to be rather low. (b) A typical HDS base $\gamma$-alumina (Ketjen fluid powder alumina, grade B) with a specific surface area of 240 m² g⁻¹ was obtained from Akzo Chemie, Ketjen catalyst division. (c) Degussa $SiO_2$ (Type Aerosil 200; surface area: 150 m² g⁻¹) was used for oxidic Co–Mo/$SiO_2$ samples, and Ketjen $SiO_2$ (fluid silica F-2; surface area 397 m² g⁻¹) was used for the sulfided catalysts. Both silicas were neutralized with ammonia before use. (d) Aqueous solutions of ammonium heptamolybdate and cobalt nitrate (both Merck A.G. products, purity grade, pro analysi) were used to impregnate the carrier materials. (e) $Co_3O_4$ was prepared by heating $Co(NO_3)_2$ at 673 K in air for 24 h. CoO was obtained by heating $Co(NO_3)_2$ in nitrogen at 1273 K *(17)*. (f) $CoAl_2O_4$, $\alpha$-$CoMoO_4$, $Fe_2(MoO_4)_3$, $Cr_2(MoO_4)_3$, $Al_2(MoO_4)_3$, and $Al_2(WO_4)_3$ were prepared by mixing stoichiometric quantities of the corresponding oxides in a ball mill and heating the mixtures at temperatures between 973 and 1273 K for 24 h ($\alpha$-$CoMoO_4$ was prepared by grinding the originally obtained $\beta$-$CoMoO_4$ in a ball mill). (g) $MoO_3$ was obtained by thermal decomposition of ammonium heptamolybdate at 873 K in air. (h) $MoS_2$ (purity > 98.5%) was obtained from Schuchardt. (i) $Co_9S_8$ was prepared by sulfiding $Co_3O_4$ at atmospheric pressure at 673 K in a $H_2S$/$H_2$ flow (volume ratio 1:6) for 4 h.

TABLE 1

List of Catalysts Studied

| | $MoO_3$ (wt%) | CoO (wt%) | Surface area ($m^2\,g^{-1}$) | Notation |
|---|---|---|---|---|
| Degussa $\gamma$-Al$_2$O$_3$ | — | — | 80 | Al–D |
| | 6 | — | 70 | Mo(6)/Al–D |
| | 9 | — | 60 | Mo(9)/Al–D |
| | 12 | — | 58 | Mo(12)/Al–D |
| | 15 | — | 51 | Mo(15)/Al–D |
| | | 2 | 74 | Co(2)/Al–D |
| | | 8 | 68 | Co(8)/Al–D |
| | 6 | 2 | — | Co(2)Mo(6)/Al–D |
| | 12 | 4 | 58 | Co(4)Mo(12)/Al–D |
| Ketjen $\gamma$-Al$_2$O$_3$ | — | — | 240 | Al–K |
| | 5 | — | — | Mo(5)/Al–K |
| | 10 | — | — | Mo(10)/Al–K |
| | 15 | — | — | Mo(15)/Al–K |
| | 20 | — | — | Mo(20)/Al–K |
| | 25 | — | — | Mo(25)/Al–K |
| | 30 | — | — | Mo(30)/Al–K |
| | 5 | 1.7 | — | Co(1.7)Mo(5)/Al–K |
| | 10 | 3.4 | — | Co(3.3)Mo(10)/Al–K |
| | 15 | 5.0 | — | Co(5)Mo(15)/Al–K |
| | 20 | 6.7 | — | Co(6.7)Mo(20)/Al–K |
| | 25 | 8.3 | — | Co(8.3)Mo(25)/Al–K |
| | 30 | 10.0 | — | Co(10)Mo(30)/Al–K |
| | 12 | | | Mo(12)/Al–K |
| | 12 | 4 | 240 | Co(4)Mo(12)/Al–K |
| Degussa SiO$_2$ | — | — | 155 | Si–D |
| | 6 | | 147 | Mo(6)/Si–D |
| | 12 | | 114 | Mo(12)/Si–D |
| | 6 | 2 | 146 | Co(2)Mo(6)/Si–D |
| Ketjen SiO$_2$ | — | — | 397 | Si–K |
| | 12 | | — | Mo(12)/Si–K |
| | 12 | 4 | — | Co(4)Mo(12)/Si–K |

(j) A commercial Ketjen Co–Mo/$\gamma$-Al$_2$O$_3$ catalyst (Type 124-1.5; surface area: 217 $m^2\,g^{-1}$) containing 12.4 wt% $MoO_3$ and 4.1 wt% CoO was also used as a reference compound.

*Catalyst preparation.* The oxidic catalyst samples were prepared according to standard sequential impregnation methods (pore volume impregnation, drying for 12 h at 383 K, and calcining for 2 h at 873 K in air) as described earlier for alumina-supported (*18*) and silica-supported (*19*) systems. Mo was always introduced first. All supported samples prepared are listed in Table 1. Ketjen HDS base alumina gave rise to a rather high fluorescence during recording of the Raman spectra. After heating the samples in oxygen for 17 h at 873 K this fluorescence was greatly suppressed.

Some oxidic samples [Mo(12)/Al–K, Co(4)Mo(12)/Al–K, Mo(12)/Si–K, and Co(4)Mo(12)/Si–K] were sulfided for 2 h in an $H_2S/H_2$ flow (volume ratio, 1:6; flow rate, 50 $cm^3$ $min^{-1}$) at atmospheric pressure and 673 K. Co–Mo/SiO$_2$

underwent an intermediate sulfiding according to the preparation method described earlier (19).

It is important to stress the fact that the catalysts were not sulfided *in situ* since there was no rotating *in situ* cell available and in the nonrotating *in situ* cell the samples would be heated too much by the laser beam. Reduction of some samples [Mo(6)/Al–D and Mo(12)/Al–D] was carried out (not *in situ*) in a hydrogen flow at 523 K for 2 h.

*Methods.* Laser Raman spectra were recorded with a Jeol JRS-1 spectrometer. This instrument was equipped with a Coherent Radiation Model 52 argon ion laser. The output power of the laser was reduced to 50–100 mW (4880-Å line). The scanning speed was usually low in the case of colored samples (10 $cm^{-1}$ $min^{-1}$), the slit width amounted to 7 $cm^{-1}$, and the sensitivity of the recording was adjusted to the intensity of the Raman scattering. In order to reduce the fluorescence and to prevent warming up of the samples, they were rotated at a speed of 1700 rpm during recording. In some cases spectra were recorded without rotation, giving rise to an increase in temperature on the spot where the laser beam hit the sample. This temperature increase strongly depends on the absorptive properties of the samples (color). A white sample such as ammonium heptamolybdate is converted into $MoO_3$ with a laser power of 100 mW within 15 min. All samples were pelletized at a pressure of 1.52 × 10⁸ N $m^{-2}$ before being mounted in the Raman spectrometer sample holder. Specific surface area and pore size distribution of some samples were derived from $N_2$ adsorption isotherms.

## RESULTS AND DISCUSSION

From the work of Cord et al. (20) and from other data presented in the literature it follows that the spectra of molybdates can be grouped according to their crystal
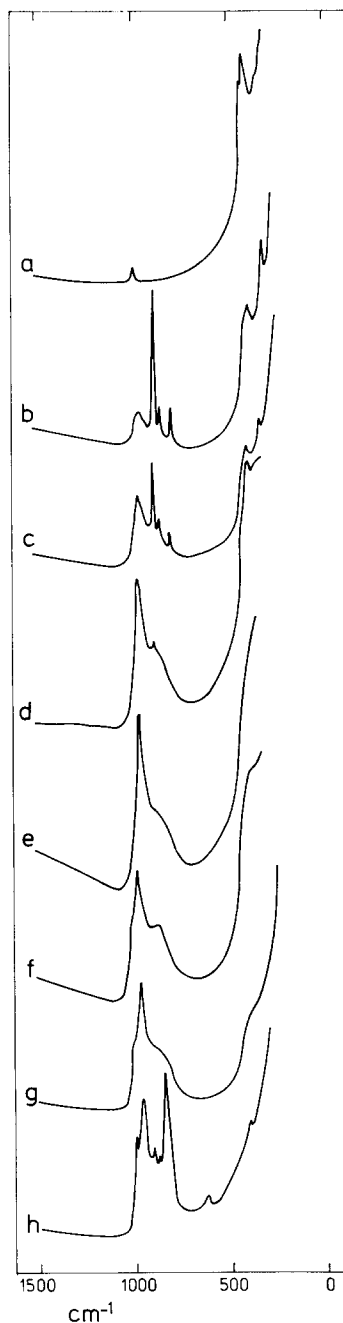


FIG. 1. Raman spectra of Mo/Al–K catalysts. (a) Carrier; (b) Mo(5)/Al–K; (c) Mo(10)/Al–K; (d) Mo(15)/Al–K; (e) Mo(20)/Al–K; (f) Mo(25)/Al–K; (g) Mo(30)/Al–K; (h) Mo(30)/Al–K. All samples except h were treated for 16 h in oxygen at 873 K. Due to fluorescence and variations in the positioning of the samples, intensities are not proportional to Mo content.
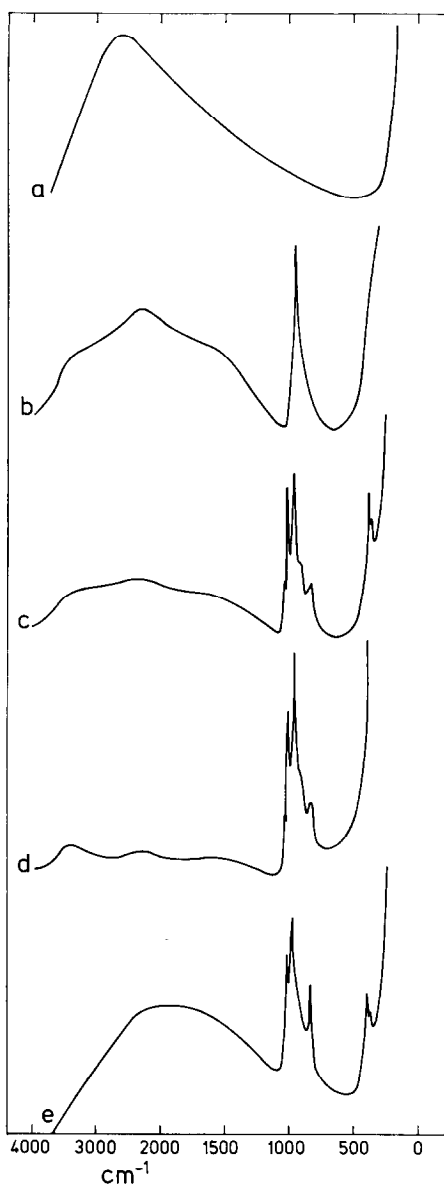
FIG. 2. Raman spectra of Mo/Al–D catalysts.
(a) Carrier; (b) Mo(6)/Al–D; (c) Mo(9)/Al–K;
(d) Mo(12)/Al–D; (e) Mo(15)/Al–D.

structure and symmetry. Compounds having the same symmetry will produce similar infrared spectra. This holds for the overall spectrum, the approximate position of the absorption bands, and the intensity of the absorptions. The exact band position is related to the Mo–O distance and

to the Mo–O bond order as was shown by Cotton and Wing (*21*). From their work it also follows that it is rather inconclusive to relate the frequency of an absorption to the presence of a terminal or bridged Mo–O bond as was done by Mitchell and Trifirò (*22*). First, one should identify identical vibrations. From the corresponding frequencies, force constants corrected for mutual interactions can be calculated and, thus, bond orders and bond distances can be calculated. The bond order is a better indication for bridged or terminal oxygens. Looking only at the frequency one has to deal with the problem that there is a considerable overlap in the frequencies of bridged and terminal oxygens. For MoO$_t$ Cotton and Wing (*21*) gave frequencies ranging from 1046 to 840 cm$^{-1}$, and for Mo–O$_b$, from 946 to 820 cm$^{-1}$. Because the assignment of the Raman lines in the spectra of pure compounds is not unambiguous, force constants cannot be calculated accurately. We therefore prefer to compare overall spectra and to relate these spectra to a certain symmetry class on the basis of data in the literature. Once the crystal structure is known it can be decided how much bridged and terminal oxygen is present.

*Oxidic Mo/γ-Al$_2$O$_3$*

In the catalyst samples the spectral features change considerably with increasing Mo content. The spectra are composed of signals arising from three to four different Mo modifications (see Figs. 1 and 2). For Mo($x$)/Al–K samples with surface coverage lower than 30% [Mo(5)/Al–K and Mo(10)/Al–K] the first type of Mo species is found. The corresponding Raman lines are remarkably sharp. Pure tetrahedral MoO$_4{}^{2-}$ as present in aqueous solutions gives a sharp strong line at about 890 cm$^{-1}$, a line at 325 cm$^{-1}$, and a weak line at 825 cm$^{-1}$. The 890 and 325 cm$^{-1}$
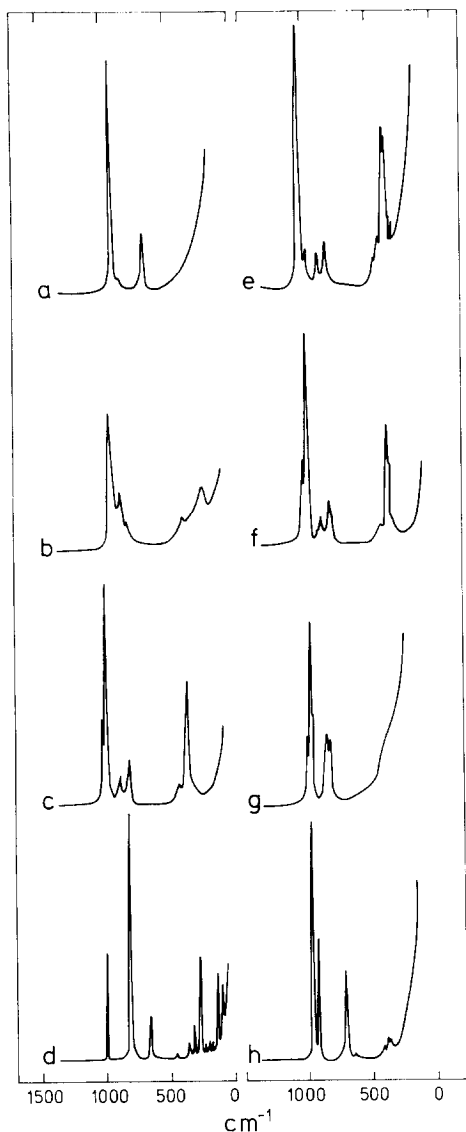
FIG. 3. Raman spectra of some selected compounds. (a) $\alpha$-CoMoO₄; (b) (NH₄)₆Mo₇O₂₄; (c) Al₂(MoO₄)₃; (d) MoO₃; (e) Al₂(WO₄)₃; (f) Al₂(MoO₄)₃; (g) Cr₂(MoO₄)₃; (h) Fe₂(MoO₄)₃.

$MoO_4$ tetrahedra in or at the alumina surface. They are most probably at the surface; otherwise $Al_2(MoO_4)_3$ formation would have resulted. Similar sharp Raman shifts were observed by Brown and Makovsky (16).

These authors also observed a broad band centered around 950 cm⁻¹, a vibration present in all our samples. In addition a shoulder at 875 cm⁻¹ is observed. The broadening of the lines indicates that we are not dealing with well-defined molybdenum compounds. The position and the intensity of the bands showed a resemblance with the Raman shifts present in $\alpha$-CoMoO₄ (see Fig. 3). The resemblance to the spectrum of $(NH_4)_6Mo_7O_{24}\cdot4H_2O$ is even better because in this case also a slight broadening can be observed. In both cases the structure of the molybdates is that of distorted octahedra (23), the distortion being of the same type. In addition both structures are bridged. In $\alpha$–CoMoO₄ the $MoO_6$ octahedra are bridged by $CoO_6$ octahedra, whereas in $(NH_4)_6$-$Mo_7O_{24}\cdot4H_2O$ the principal bridging occurs via the molybdate octahedra. It has been found that, when the degree of polymerization of molybdates changes from hepta to octa, a small shift in the Raman lines as well as line broadening occurs (24). In view of the band position and the broadening of the band as observed in Mo/$\gamma$-Al₂O₃ samples we conclude that the broad band at 950 cm⁻¹ is due to a bridged or a two-dimensional polymeric form of distorted molybdate octahedra. This con-
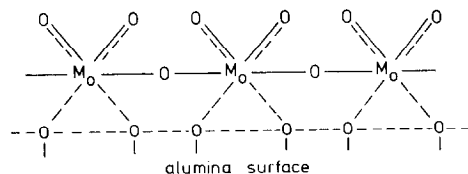


FIG. 4. Possible structure of polymeric molybdate. In this picture a certain competition between the Mo–O surface bonds, dotted lines, and the protruding Mo–O bonds is presumed.

lines are both observed in the supported samples but the 825 cm⁻¹ seems to split into two, viz., one at 840 cm⁻¹ and another at 800 cm⁻¹. A slight distortion of the tetrahedral symmetry is sufficient to explain the splitting of this 825 cm⁻¹ band. We therefore conclude that the sharp lines present at low coverages belong to isolated

clusion is in accordance with the findings of Giordano *et al.* (*25*). From uv reflectance spectroscopy (*26*) it follows that the main fraction of the molybdenum is tetrahedrally surrounded by oxygen in $Mo/\gamma-Al_2O_3$ at medium surface coverages. As Cord *et al.* (*20*) pointed out, the distortion of the octahedral symmetry is such that a nearly perfect tetrahedral coordination results. We prefer to speak of octahedra although two oxygens are at large distances (0.23 nm) and these do not influence the Mo very much. The bridging between the molybdate octahedra is such that two terminal oxygens are present, two oxygen ions are used for bridging, and two oxygen ions are used for interaction with the alumina surface. It cannot be ruled out that the latter two oxygens form part of the alumina lattice. This picture as shown in Fig. 4 is very similar to the one presented by Giordano *et al.* (*25*). Comparing catalyst samples Mo(5)/Al–K, Mo(10)/Al–K, and Mo(15)/Al–K increasing in Mo content, one has the impression that the polymeric form of molybdate grows at the expense of the monomeric species. In order to check this, we recorded a Raman spectrum of a 1:1 mixture of Mo(25)/Al–K and Mo(5)/Al–K.

If the absolute quantity of monomeric molybdate is constant for all samples of the $Mo(x)/Al–K$ series, one would expect to find for this mixture an intensity of the sharp lines that is about equal to the intensity found in the spectrum of Mo(15)/Al–K. However, the intensity of the sharp line at 890 $cm^{-1}$ in the mixture was at least fourfold the intensity of the line found in Mo(15)/Al–K. This result leads to the conclusion that the monomeric molybdates do indeed combine to polymeric molybdate when the Mo concentration is increased.

The Mo(9)/Al–D and Mo(12)/Al–D samples show additional lines in comparison with the Mo(6)/Al–D spectrum (see Fig. 2). The line or combination of lines slightly above 1000 $cm^{-1}$ is particularly peculiar. In the Mo(20)/Al–K, Mo(25)/Al–K, and Mo(30)/Al–K samples these lines appear as a shoulder around 1010 $cm^{-1}$. Comparison with the spectra of pure compounds shows that we are dealing with $Al_2(MoO_4)_3$ (Fig. 3). To our knowledge the structure of this compound is not reported in the literature. It is, however, stated that $Al_2(MoO_4)_3$, $Cr_2(MoO_4)_3$, and $Fe_2(MoO_4)_3$, as well as $Al_2(MoO_4)_3$ and $Al_2(WO_4)_3$, are isomorphous (*15*, *27*). The Raman spectra as given in Fig. 3 confirm this statement. The structure of $Al_2(WO_4)_3$ given by Craig and Stephenson (*28*) and by de Boer (*29*) is identical to the proposed structure of $Fe_2(MoO_4)_3$ (*30*). A tetrahedral surrounding of Mo by oxygen and an octahedral surrounding of the cation without terminal oxygens was proposed. Therefore, it is concluded that the structure of $Al_2(MoO_4)_3$ is based on $MoO_4$ tetrahedra and $AlO_6$ octahedra ions and that in this structure terminal oxygens are absent. It is therefore unlikely that $Al_2(MoO_4)_3$ as found in the catalyst is a "two-dimensional surface complex." $Al^{3+}$ octahedral sites from the $Al_2O_3$ spinel lattice play an essential part in the formation of bulk $Al_2(MoO_4)_3$; moreover, as no terminal oxygens are present, the molybdate tetrahedra must be formed inside the alumina lattice, probably on the subsurface.

Further increase of surface coverage results in samples like Mo(15)/Al–D and Mo(30)/Al–K (see Figs. 1 and 2) having two sharp lines at 990 and 820 $cm^{-1}$, a band at 670 $cm^{-1}$, and another band at 375 $cm^{-1}$. These lines can be attributed to "free" $MoO_3$ on top of the alumina surface, as the position and the relative intensities are the same for $MoO_3$. On prolonged heat treatment [sample Mo(30)/Al–K was heated for 17 h in oxygen at 873 K; sample Mo(15)/Al–D for 2 h at 1073 K] these bands disappear from the spectrum due to sublimation of the $MoO_3$.

The formation of "free" $MoO_3$ at higher coverages is in accordance with the results of Giordano et al. (25).

Other investigators also describe the formation of "free" $MoO_3$ (26). In this case the structure of the compound consists of $MoO_6$ octahedra as was reported by Kihlborg (31). At this point it is interesting to note the influence of heat treatment on the structure of Mo in Mo/$\gamma$-Al₂O₃ samples. Except for the disappearance of $MoO_3$ no other influence was noted in the Degussa alumina samples, not even after prolonged heating for 15 h at 1073 K. In the Ketjen alumina samples heat treatment for 17 h at 873 K in oxygen has been used in order to reduce the fluorescence. In those samples where spectra could be recorded without this heat treatment, identical spectra were obtained except for "free" $MoO_3$ and of course fluorescence. Heating of Ketjen alumina with low-Mo-content compounds for a longer time at 1023 K influences the amount of monomeric molybdate in favor of polymeric molybdate, which is formed slowly. It is justified therefore to treat the Ketjen alumina samples as normal HDS catalyst precursors, despite the fact that they are heated for 17 h at 873 K.

In Fig. 5a the various Mo species present in the supported samples are shown schematically. At low surface coverages monomeric molybdate tetrahedra are found. At medium coverages the empty spaces between the solitaire molybdates become filled, resulting in formation of polymolybdate with distorted octahedra. Further increase in surface coverage results in the formation of subsurface $Al_2(MoO_4)_3$ in which $Mo^{6+}$ is tetrahedrally surrounded and $Al^{3+}$ takes octahedral positions. At very high coverages "free" $MoO_3$ is formed consisting of strongly distorted octahedra. This "free" $MoO_3$ can be removed from the surface by sublimation. This scheme greatly resembles the detailed structural model presented by Giordano et al. (25).
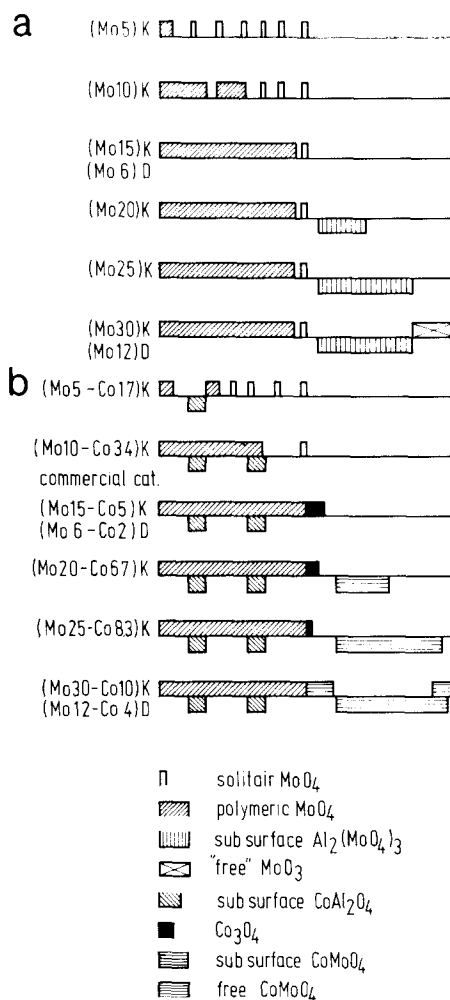
FIG. 5. (a) Upper six diagrams: coverage of the surface of alumina with the different molybdenum species, depending on the degree of surface coverage. (b) Lower six diagrams: coverage of the surface of alumina with the different molybdenum and cobalt species, depending on the degree of surface coverage.

It is remarkable that it could be derived on the basis of results obtained using one technique, showing that Raman spectroscopy is a valuable tool in studying the structure of catalysts.

If corrections for the differences in surface areas are made, the differences between the two types of alumina are small, the main difference being that, in Degussa alumina, the formation of $Al_2(MoO_4)_3$ is

more pronounced. This is probably due to the differences in texture and/or impurity content, for instance, $SiO_2$ in the two aluminas. Degussa alumina has a bidisperse pore structure, a small fraction of micropores, and a large fraction of pores 12.5 nm in diameter. Ketjen alumina has pores in the range of 3.5–7.0 nm in diameter. The molybdate present in micropores is already surrounded by $Al_2O_3$ at "three" sites, and the formation of $Al_2(MoO_4)_3$ might be facilitated through this surrounding.

*Oxidic Co/γ-Al₂O₃*

In the spectra recorded for Co(y)/Al–D samples one Raman line was clearly visible (see Fig. 6). Only in the case of low fluorescence [Co(8)/Al–D] could a second relatively weak and broad line at about 530 cm⁻¹ be observed. This line at 690 cm⁻¹ is also present in α-CoMoO₄ and Co₃O₄,



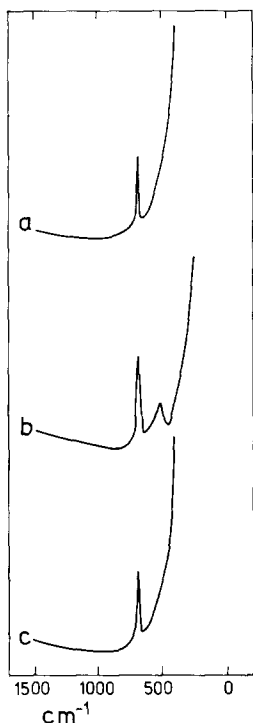FIG. 6. Raman spectra of Co/Al–D catalysts. (a) Co(2)/Al–D; (b) Co(8)/Al–D; (c) Co₃O₄.

compounds differing in symmetry. In α-CoMoO₄, the Co²⁺ ions are situated in octahedra, whereas in Co₃O₄ the Co²⁺ is tetrahedrally coordinated (*32*). Both CoO (CoO₆ octahedra) and CoAl₂O₄ (CoO₄ tetrahedra) gave no detectable Raman signal under our experimental conditions. Apparently they do not have disturbed symmetries. Obviously the line at 690 cm⁻¹ as present in α-CoMoO₄ and Co₃O₄ is due to a Co–O stretching mode. As this line is also found in the Co(y)/Al–D catalysts, at least part of the Co²⁺ is in a Raman-detectable form. The color of both CoO and Co₃O₄ is nearly black and so is that of Co(8)/Al–D, whereas the color of Co(2)/Al–D is blue gray. The blue component in the 2% sample is probably due to Co²⁺ ions in a spinel system like CoAl₂O₄ (*33*). Thus we have a mixture of CoAl₂O₄ and Co₃O₄. At higher coverages the Co₃O₄ content increases to such an extent that the color of CoAl₂O₄ becomes invisible. The presence of CoO is unlikely as it is not a stable component at the temperature of preparation of the Co(y)/Al–D samples (*34*).

*Oxidic Co–Mo/γ-Al₂O₃*

Introducing Co into the Mo(x)/Al catalysts (at such a concentration that the CoO/MoO₃ weight percentage ratio is 1/3) results in the following effects (see Fig. 7). Blue-colored samples were obtained. The monomeric MoO₄ phase in the low coverage samples is converted partly into the polymolybdate MoO₆ phase. In Co(3.7)-Mo(10)/Al–K, the monomeric MoO₄ phase is no longer observed. Based on the color of the samples one should expect the presence of either CoAl₂O₄ or CoMoO₄. No Raman lines characteristic of CoMoO₄ (960 and 690 cm⁻¹) can be observed. Thus in low coverage samples Co²⁺ is present in the form of CoAl₂O₄ in the lattice of alumina. The formation of a polymeric phase of MoO₆ octahedra under the in-

fluence of Co was also suggested by Grimblot and Bonnelle (*35*) on the basis of ESCA and TGA measurements. In this case the $Co^{2+}$ is supposed to be present in a tetrahedral configuration inside the alumina lattice, and every Co interacts with an ensemble of four combined molybdate ions on the surface. In fact this is an elaborated picture of the monolayer model described by Schuit and Gates (*1*).

At medium Co concentrations (e.g., Co(2)Mo(6)/Al–D and Co(5)Mo(15)/Al–K) a shift appears at 690 cm⁻¹. The color of this sample is still blue. It is very unlikely that the Raman shift at 690 cm⁻¹ is caused by $CoMoO_4$, because the strongest line for this compound at 960 cm⁻¹ is absent. We therefore conclude that in these samples, beside $CoAl_2O_4$ a small amount of microcrystalline $Co_3O_4$ is also present. This is in accordance with data reported in the literature (*19, 33, 36–38*).

When the Co concentration is increased further [i.e., high surface coverage: Co(6.7)Mo(20)/Al–K, Co(8.3)Mo(25)/Al–K, Co(10)Mo(30)/Al–K, and Co(4)-Mo(12)/Al–D], the 950 cm⁻¹ band (poly-molybdate phase) is doubled as a result of the presence of a line at 960 cm⁻¹. Remarkably the relative intensity of the line at 690 cm⁻¹ decreases as the Co concentration increases. In the spectrum recorded from Co(10)Mo(30)/Al–K the intensity ratios of the 960 cm⁻¹ line and the 690 cm⁻¹ line are approximately in accordance with the ratio found for pure $CoMoO_4$. Apparently the $Co_3O_4$ concentration decreases and the $CoMoO_4$ concentration increases when the surface coverage is increased. The samples are still intensely blue colored, indicating that $CoAl_2O_4$ is probably present also (*37*). It is noteworthy that $CoMoO_4$ is apparently formed at the expense of the $Al_2MoO_4$ present in the $Mo/\gamma$-$Al_2O_3$ samples used for the preparation of the Co-containing catalysts.

The spectrum of the commercial Ketjen

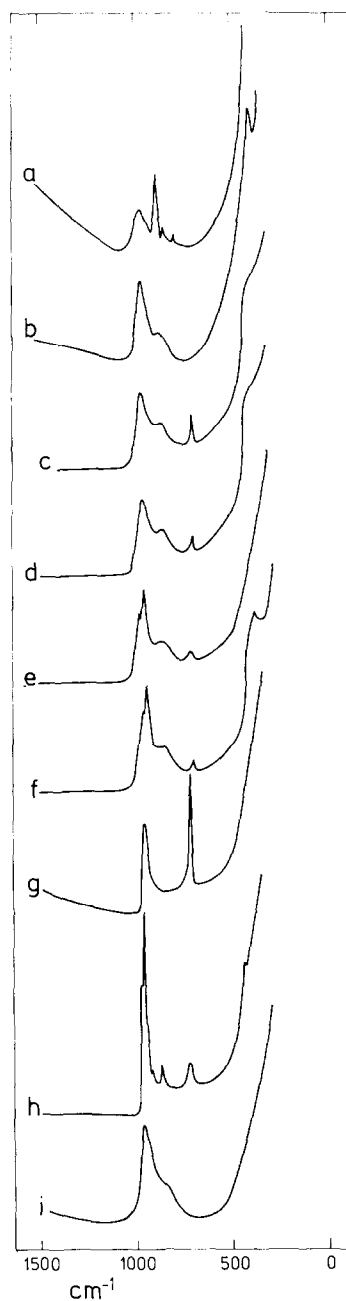Co–Mo/γ-Al₂O₃ catalyst containing 12.4 wt% $MoO_3$ and 4.1 wt% $CoO$ shows



FIG. 7. Raman spectra of cobalt and molybdenum on Degussa and Ketjen alumina. (a) Co(1.7)Mo(5)/Al–K; (b) Co (3.4)Mo(10)/Al–K; (c) Co(5)Mo(15)/Al–K; (d) Co(6.7)Mo(20)/Al–K; (e) Co(8.3)-Mo(25)/Al–K; (f) Co(10)Mo(30)/Al–K; (g) Co(2)-Mo(6)/Al–D; (h) Co(4)Mo(12)/Al–D; (i) Co(4)-Mo(12)/Al–K, commercial Ketjen catalyst.

Raman lines that can be attributed to polymeric $MoO_6$ octahedra. There is no indication of the presence of any other Mo compounds, in accordance with the findings of other investigators (33). The absence of the strongest $CoMoO_4$ line (960 cm$^{-1}$) and the 690 cm$^{-1}$ line ($CoMoO_4$ or $Co_3O_4$) and the fact that the catalyst is blue justify the conclusion that Co is exclusively present as $Co^{2+}$ ions in the alumina lattice in a form comparable to that of $CoAl_2O_4$.

In Fig. 5b the effect of Co introduction into oxidic Mo($x$)/Al catalysts is given schematically. At low surface coverages $Co^{2+}$ ions present in the $\gamma$-alumina surface or subsurface layers as $CoAl_2O_4$ facilitate the transformation of isolated tetrahedral $MoO_4$ species into a polymolybdate phase (this is a monolayer of $MoO_6$ octahedra on top of the alumina surface). At medium surface coverages an additional Co phase, viz., $Co_3O_4$, is formed. In this range of Mo and Co concentrations no indication for the formation of a known Co/Mo compound was obtained. This strongly suggests that there is only a moderate interaction [for instance, of the type described by Grimblot and Bonnelle (35)] between the Co and Mo species present in these Co–Mo/$\gamma$-Al$_2$O$_3$ catalysts. At higher coverages the subsurface $Al_2(MoO_4)_3$ phase and "free" $MoO_3$ on top of the monolayer are converted into $CoMoO_4$. The structure of oxidic Co–Mo/Al described above is in some respect different from that given by Ratnasamy et al. (39), based on findings from reduction (TGA and DTA), acidity, and activity measurements, as well as on infrared spectra. However, we tend to believe that especially for fresh nonreduced oxidic samples laser Raman spectroscopy results in more direct information about the nature of Co and Mo present in these catalysts. For Co($y$)Mo($x$)/Al–D and Co($y$)Mo($x$)/Al–K the results are similar provided that the surface coverages are comparable (in Fig. 7 compare curve c

with curves g, f, and h). This was also the case for the commercial Ketjen Co(4)Mo(12)/Al–K and the laboratory-prepared Co(3.4)Mo(10)/Al–K catalysts, indicating again that the pretreatment in oxygen for 17 h at 873 K, treatment to which the laboratory-prepared samples were subjected, has not affected the catalyst structure significantly (the commercial catalyst was not subjected to this treatment).

The earlier finding (19, 40) that the commercial Ketjen catalyst has optimum Co and Mo concentrations with respect to thiophene HDS activity and the observation that in this catalyst Mo is mainly present in the polymolybdate phase (Co induces the formation of additional polymolybdate) strongly suggest that this phase is the most important precursor for the main active compound ($MoS_2$) in sulfided Co–Mo/$\gamma$-Al$_2$O$_3$ HDS catalysts. Additional support for this suggestion can be derived from previously published data (19) showing that addition of 4 wt% CoO to Mo(4)/Al–K increases the thiophene HDS activity considerably. On the basis of the model described here this phenomenon can be explained by an increase in the polymolybdate concentration and a decrease in the isolated $MoO_4$ species as a result of Co introduction. The isolated $MoO_4$ species in samples with low surface coverages are probably highly resistant to reduction by hydrogen as well as to sulfidation by $H_2S/H_2$, and they are very probably the same as the phase A sites mentioned by Ratnasamy et al. (39). Based on thiophene HDS and olefin hydrogenation activity measurements, it was concluded earlier (19) that these $MoO_4$ tetrahedra species are preserved to a certain extent in oxidic and sulfided Ketjen and laboratory-prepared Co(4)Mo(12)/Al–K catalysts. Their presence is not observable by means of Raman spectroscopy in the commercial catalyst and only small peaks in the spectra of some laboratory-prepared

catalysts might be attributed to these tetrahedra. Therefore their concentration is probably very low.

*Reduction Experiments*

Reduction (not *in situ*) of the $Mo(x)/Al$ samples in hydrogen at 523 K for 1 h results in disappearance of the Raman lines ascribed to polymolybdate species. At the same time the samples show a very strong fluorescence level, the lines characteristic of $MoO_4$ tetrahedra cannot be detected, and the "free" $MoO_3$ phase is no longer detectable. Note that $MoO_2$ does not show Raman activity. $Al_2(MoO_4)_3$ is the only compound clearly observable in reduced samples (bands at 1000 and 375 cm⁻¹). Samples which originally did not contain $Al_2(MoO_4)_3$-like species surprisingly also showed a band at 1000 cm⁻¹ after reduction.

*Oxidic Mo/SiO₂ and Co–Mo/SiO₂*

As can be seen in Fig. 8 the spectra recorded for $Mo(6)/Si–D$ and $Mo(12)/Si–D$ almost show merely the lines characteristic for "free" $MoO_3$. These spectra also indicate the presence of small amounts of poly-$MoO_6$ species. The intensities of the $MoO_3$ lines in these spectra are about equal despite the fact that they are recorded at sensitivities that differ by a factor of 20. This strongly suggests that $Mo(12)/Si–D$ contains much more than twice the amount of "free" $MoO_3$ present in $Mo(6)/Si–D$ and that consequently in the latter catalyst a substantial fraction of the Mo is present as polymolybdate. The observed differences are very likely to be caused by differences in Raman cross sections of "free" $MoO_3$ and polymolybdate. It is noteworthy that the color of the $Mo(x)/Si–D$ samples turned from white to blue immediately after exposure to the laser beam, even when the samples were rotated. This points to the formation of molybdenum blue, which is a reduced form of molybdenum oxide containing
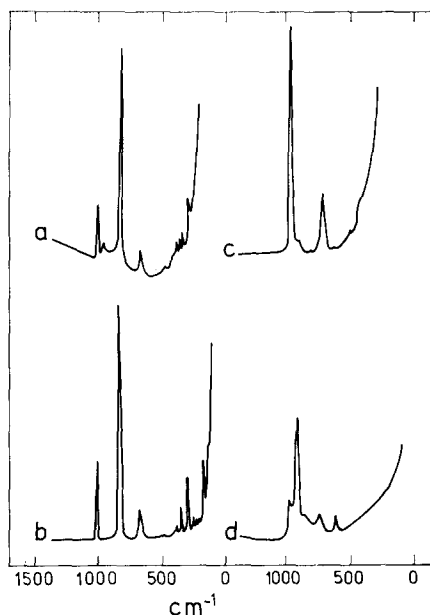


FIG. 8. Raman spectra of Mo and Co on silica catalysts. (a) $Mo(6)/Si–D$; (b) $Mo(12)/Si–D$; (c) $Co(2)Mo(6)/Si–D$; (d) $Co(4)Mo(12)/Si–K$.

molybdenum ions with valences between 4 and 6 (*41*).

Addition of Co to $Mo(6)/Si–D$ resulted in formation of $\alpha$-$CoMoO_4$ (see Figs. 3a and 8c). After impregnation of Ketjen silica with Mo and Co [$Co(4)Mo(12)/Si–K$] a violet-gray catalyst was obtained. It was concluded earlier (*19*) that this catalyst contains $\beta$-$CoMoO_4$ (violet modification) and $Co_3O_4$ (black). The Raman spectrum of $Co(4)Mo(12)/Si–K$ (see Fig. 8d) indicates the presence of $Co_3O_4$ and shows a good resemblance to the spectrum of the metastable high-temperature $CoMoO_4$ modification as given by Cord *et al.* (*20*). It is noteworthy that Co addition led to the disappearance of the "free" $MoO_3$ Raman scattering. This might indicate that $CoMoO_4$ formation occurs preferentially via interaction of Co with the "free" $MoO_3$ phase, which was originally present in the $Mo/SiO_2$ samples. From the Raman data it can be concluded that silica interacts with Mo species to a lesser extent than does alumina. Both
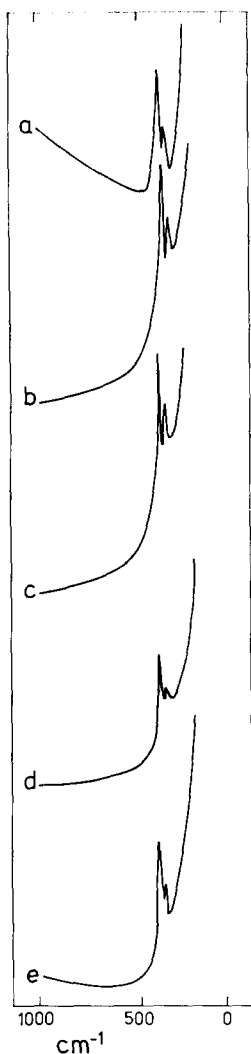
FIG. 9. Raman spectra of sulfided catalysts.
(a) Mo(12)/Al–K; (b) Co(4)Mo(12)/Al–K; (c)
Mo(12)/Si–K; (d) Co(4)Mo(12)/Si–K; (e) MoS₂-
(10)/Al–K.

silicas show less interaction with the Mo
species than does alumina. "Free" MoO₃
or crystalline modifications of CoMoO₄
are formed at lower surface coverage than
in the case of alumina-supported catalyst
systems. This agrees with the data published by Castellan *et al.* (*42*) and de Beer
*et al.* (*19*).

*Effect of Sample Rotation*

So far the structural model of Co–Mo/
γ-Al₂O₃ catalysts as derived from Raman

spectroscopy is consistent with data derived
via a number of other techniques. However, the Raman data were found to be
dependent on the way in which the spectra
were recorded, viz., with or without sample
rotation. With rotation the samples were
heated only slightly above room temperature. Nonrotating samples were heated
much more and the temperature in most
cases was above 523 K. This induces a
strong fluorescence in the samples and it
becomes difficult to record Raman spectra.

In those cases in which we were able
to record a spectrum of a catalyst sample
without rotation, the spectrum was different from the spectrum at "room temperature." It seems as if, as a result of
the temperature increase, the polymeric
molybdate is converted in a similar way
as mentioned before for bulk (NH₄)₆Mo₇-
O₂₄·4H₂O (see Experimental Methods).
In the latter case bulk MoO₃ is formed
whereas polymeric molybdate is converted
into a structure resembling aluminium
molybdate. Even prolonged heat treatment
in an oven at 1073 K could not induce
this change. Preliminary experiments with
the commercial Ketjen catalyst have shown
that the conversion under the influence
of the laser beam is reversible. Experiments will be performed to elucidate these
effects further.

*Sulfided Catalysts*

Preliminary experiments have been carried out with H₂S/H₂ sulfided alumina and
silica-supported catalysts, viz., Mo(12)/
Al–K, Co(4)Mo(12)/Al–K, Mo(12)/Si–K,
and Co(4)Mo(12)/Si–K. The spectra are
given in Fig. 9. Although these catalysts
were not sulfided *in situ* (i.e., they were
exposed to air after sulfiding) only Raman
shifts (405 and 380 cm⁻¹) characteristic
of bulk MoS₂(11) were observable, as is
also shown by Brown and Makovsky (*16*).
As shown in Fig. 9 there was no significant
difference between these spectra and the
one recorded for a mechanical mixture of

bulk MoS$_2$ (10 wt%) and Ketjen $\gamma$-Al$_2$O$_3$ [MoS$_2$(10)/Al–K]. No evidence of the presence of Co$_9$S$_8$, MoS$_3$, oxomolybdenum, oxocobalt, and oxosulfomolybdenum or oxosulfocobalt species could be obtained from these spectra. These results again (5, 19) demonstrate that for sulfided samples the influence of the support on the actual active catalyst structure is much weaker than for oxidic samples.

## CONCLUSIONS

From the data presented above it is concluded that laser Raman spectroscopy is very useful in studies of fresh oxidic HDS catalyst precursors. Raman spectra clearly distinguish between Mo and Co phases present in these catalysts. Relations between the concentration of some of these phases and catalytic activity for certain reactions may be worked out via quantitative Raman spectroscopy studies.

Further studies could also be made, for instance with respect to the influence of sodium or silica on the nature and distribution of the Mo species present on the alumina carrier surface. It also seems worthwhile to study the effect of partial reduction by hydrogen on oxidic samples as well as the effect of H$_2$S/H$_2$ sulfidation by means of in situ Raman techniques.

## ACKNOWLEDGMENTS

## REFERENCES

1. Schuit, G. C. A., and Gates, B. C., AIChE J. 19, 417 (1973).
2. Grange, P., and Delmon, B., J. Less-Common Metals 36, 353 (1974).
3. Amberg, C. H., J. Less-Common Metals 36, 339 (1974).
4. de Beer, V. H. J., and Schuit, G. C. A., Ann. N. Y. Acad. Sci. 272, 61 (1976).
5. de Beer, V. H. J., and Schuit, G. C. A., in "Preparation of Catalysts" (B. Delmon,

P. A. Jacobs, and G. Poncelet, Eds.), p. 343. Elsevier, Amsterdam, 1976.
6. van Stam, C., Internal report TNO.
7. Cooney, R. P., Curthoys, G., and Tam, N. T., Advan. Catal. 24, 293 (1975).
8. Oganowski, W., Hanuza, J., Jezowska-Trzebiatowska, B., and Wrzyszcz, J., J. Catal. 39, 161 (1975).
9. Müller, A., Weinstock, N., and Schulze, H., Spectrochim. Acta 28A, 1075 (1972).
10. Leroy, M. J. F., Burgard, M., and Müller, A., Bull. Soc. Chim. Fr. 4, 1183 (1971).
11. Wieting, T. J., and Verble, J. L., Phys. Rev. B 3, 4286 (1971).
12. Chen, J. M., and Wang, C. S., Solid State Commun. 14, 857 (1974).
13. Stevens, G. C., and Edmonds, T., J. Catal. 37, 544 (1975).
14. Villa, P. L., Trifirò, F., and Pasquon, I., React. Kinet. Catal. Lett. 1, 341 (1974).
15. Pott, G. T., and Stork, W. H. J., in "Preparation of Catalysts" (B. Delmon, P. A. Jacobs, and G. Poncelet, Eds.), p. 537. Elsevier, Amsterdam, 1976.
16. Brown, F. R., and Makovsky, L. E., Appl. Spectrosc. 31, 44 (1977).
17. Brauer, G., "Handbuch der Preparativen Anorganische Chemie Ferd," p. 1134. Enkel Verlag, Stuttgart, 1954.
18. de Beer, V. H. J., van Sint Fiet, T. H. M., van der Steen, G. H. A. M., Zwaga, A. C., and Schuit, G. C. A., J. Catal. 35, 297 (1974).
19. de Beer, V. H. J., van der Aalst, M. J. M., Machiels, C. J., and Schuit, G. C. A., J. Catal. 43, 78 (1976).
20. Cord, A. P., Courtine, P., and Pannetier, G., Spectrochim. Acta 28A, 1601 (1972).
21. Cotton, F. A., and Wing, R. M., Inorg. Chem. 4, 867 (1965).
22. Mitchell, P. C. H., and Trifirò, F., J. Chem. Soc. A, 3183 (1970).
23. Lindquist, I., Ark. Kemi 2, 325 (1951).
24. Aveston, J., Anacker, E. W., and Johnson, J. S., Inorg. Chem. 3, 735 (1964).
25. Giordano, N., Bart, J. C. J., Vaghi, A., Castellan, A., and Martinotti, G., J. Catal. 36, 81 (1975).
26. Ashley, J. H., and Mitchell, P. C. H., J. Chem. Soc. A, 2730 (1969).
27. Nassau, K., Levinstein, H. J., and Loiacono, G. M., J. Phys. Chem. Solids 26, 1805 (1965).
28. Graig, D. C., and Stephenson, N. C., Acta Crystallogr. Sect. B 24, 1250 (1968).
29. de Boer, J. J., Acta Crystallogr. Sect. B 30, 1878 (1974).
30. Plyasova, L. M., Klevsova, R. F., Borisov, S. V., and Kefeli, L. M., Dokl. Akad. Nauk USSR 167, 84 (1966).

*31.* Kihlborg, L., *Ark. Kemi* **21**, 357 (1963).

*32.* Cossee, P., and van Arkel, A. E., *J. Phys. Chem. Solids* **15**, 1 (1960).

*33.* Lo Jacono, M., Cimino, A., and Schuit, G. C. A., *Gazz. Chim. Ital.* **103**, 1281 (1973).

*34.* Nicholls, D., *in* "Comprehensive Inorganic Chemistry" (J. C. Bailar, Ed.), Vol. 3, p. 1071. Pergamon Press, Oxford, 1973.

*35.* Grimblot, J., and Bonnelle, J. P., *J. Electron Spectrosc. Relat. Phenom.* **9**, 449 (1976).

*36.* Ashley, J. H., and Mitchell, P. C. H., *J. Chem. Soc. A*, 2822 (1968).

*37.* Keeling, R. O., Jr., *Develop. Appl. Spectrosc.* **2**, 263 (1962).

*38.* Ratnasamy, P., Mehrotra, R. P., and Ramaswamy, A. V., *J. Catal.* **32**, 63 (1974).

*39.* Ratnasamy, P., Ramaswamy, A. V., Banerjee, K., Sharma, D. K., and Ray, N., *J. Catal.* **38**, 19 (1975).

*40.* de Beer, V. H. J., van Sint Fiet, T. H. M., Engelen, J. F., van Haandel, A. C., Wolfs, M. W. J., Amberg, C. H., and Schuit, G. C. A., *J. Catal.* **27**, 357 (1972).

*41.* Rollinson, C. L., *in* "Comprehensive Inorganic Chemistry" (J. C. Bailar, Ed.), Vol. 3, p. 737. Pergamon Press, Oxford, 1973.

*42.* Castellan, A., Bart, J. C. J., Vaghi, A., and Giordano, N., *J. Catal.* **42**, 162 (1976).